Appendix A

Forward modeling

Forward Modeling

The mater concluded in this research is based on Fagin (1991), and Osiris User's manual (1993).

Modeling really aims to create geophysical models and set several environments to understand and explain them better as a guideline processing to any exploratory action. The modeling in general involves with four problems: *representation, measurement, estimation, and validation.* The *first one* deals with how something should be modeled. The *second one* deals with which physical quantities should be measured and how they should be measured. The *third one* deals with the determination of those physical properties that cannot be measured from those that can be measured. The *fourth one* deals with demonstrating confidence in the model. In practice, the usual philosophy is that if the results from the model are favorable, then the model is adequate and accepted. If predictions or results from the model yield unsatisfying results, then model is modified and recalculated.

There are two main types of modeling, *Forward and Inverse modeling. The former*, is conducted by predicting the seismic signal that develop from a particular depth model, comparing these reflections with the appropriate real data, determining whether the theoretical response signal compatible with the real signal or not, if not, the model is then modified. *The latter*, in opposite way, is carried out by processing the observed seismic data and defining the structure from a seismic section in time and directly obtaining the subsurface structure in depth. It can be noted that the difference between forward and inverse modeling is only their input and output (Figure A-1).

For the Osiris application used in this research, it is well-known software and has been developed and used by Odegaard & Danneskoild-Samsoe ApS, Copenhagen, Denmark, in the consultantcy department since 1985. It is also available as a modeling module (STRAT) in the seismic processing package named Geovecteur of Compagnie Generale de Geophysique (CGG), France, which was by Odegaard & Danneskoild-Samsoe. Its package includes many features such as, Seismic shot record simulation, Vertical seismic profiling (VSP) and offset VSP simulation, Visco-acoustic, visco-elastic and visco-transverse isotropic layers, Frequency spectra analysis, Transmission loss analysis, Wavenumber spectra analysis, Receiver array simulation, Decomposition of the wavefield into Primary and sheared-waves, and upgoing and downgoing waves, Source type option, Wavelet (source signature) type options, SEG-Y format, plotter, and printer support.

This software basically used Osiris method (Figure A-2) for solving 2-D and 3-D wave equation. Some examples of modeling works created by Osiris are presented in Figure A-3 whereas the scheme concerned in this research is the seismic shot record simulation shown in Figure A-4. Given an input model accompanied by its acquisition and calculation parameters, Osiris software was used to simulate the synthetic seismic data for an arbitrary horizontally stratified medium at selected receiver locations

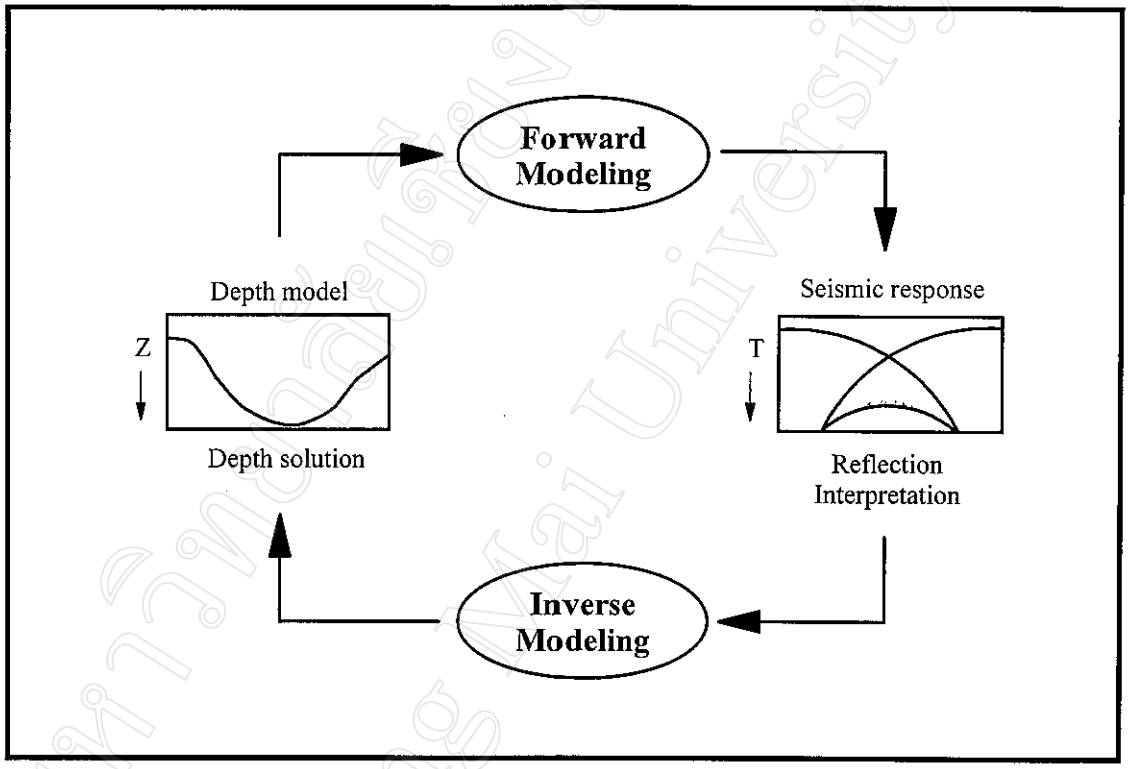

Figure A-1 Concept of Forward and Inverse modeling (Fagin, 1991)

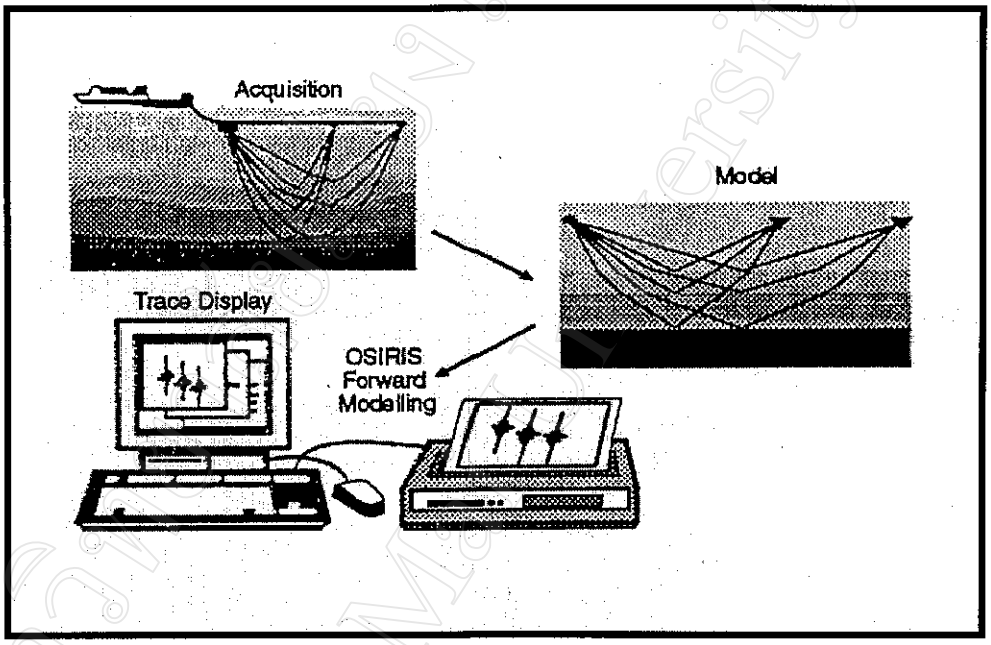

Figure A-2 The basic principle of Osiris (Osiris User's manual)

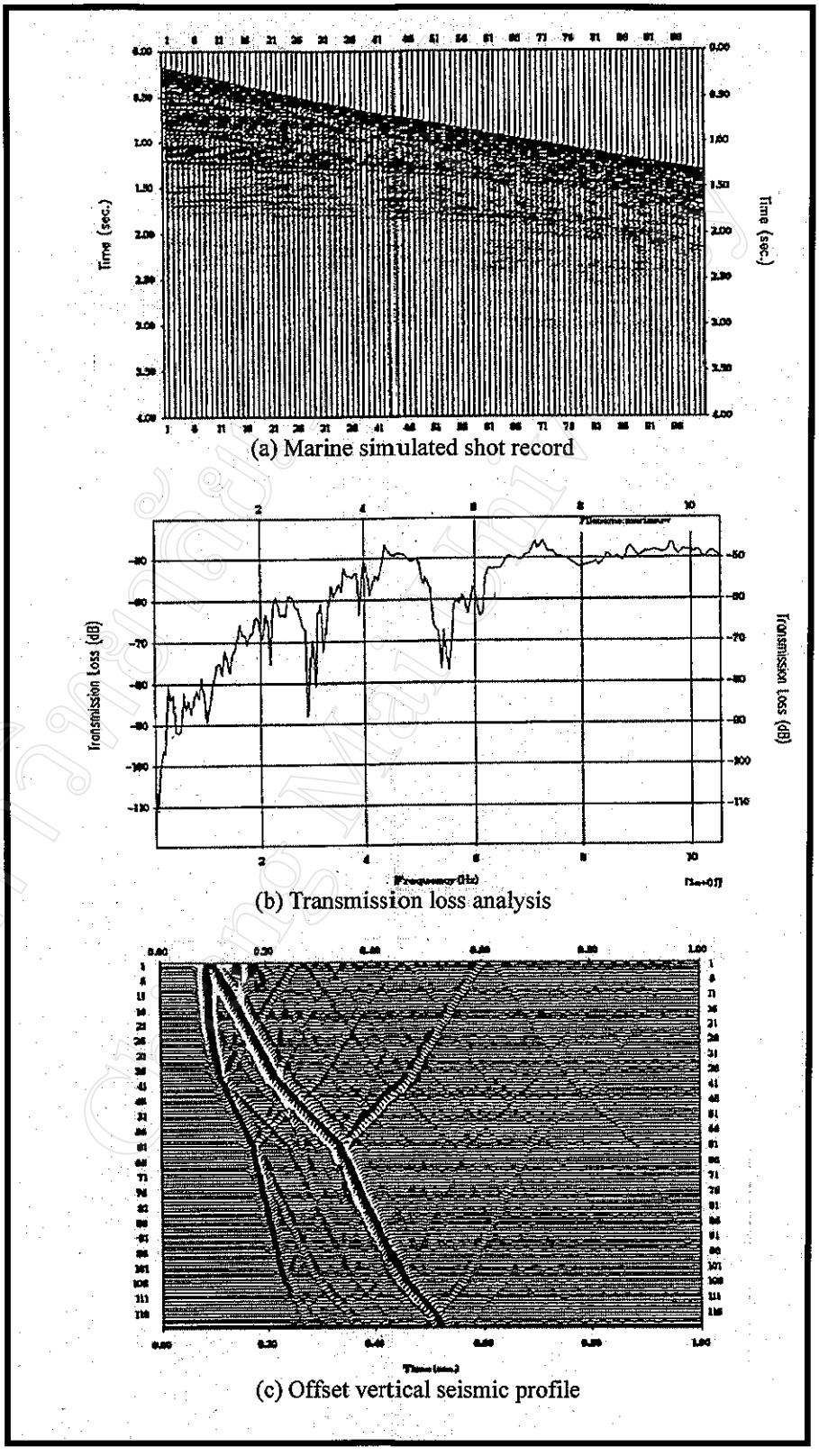

(a) Marine simulated shot record

(b) Transmission loss analysis

(c) Offset vertical seismic profile

Figure A-3 Examples of performances generated by Osiris modeling software (Modified after Osiris user's manual)

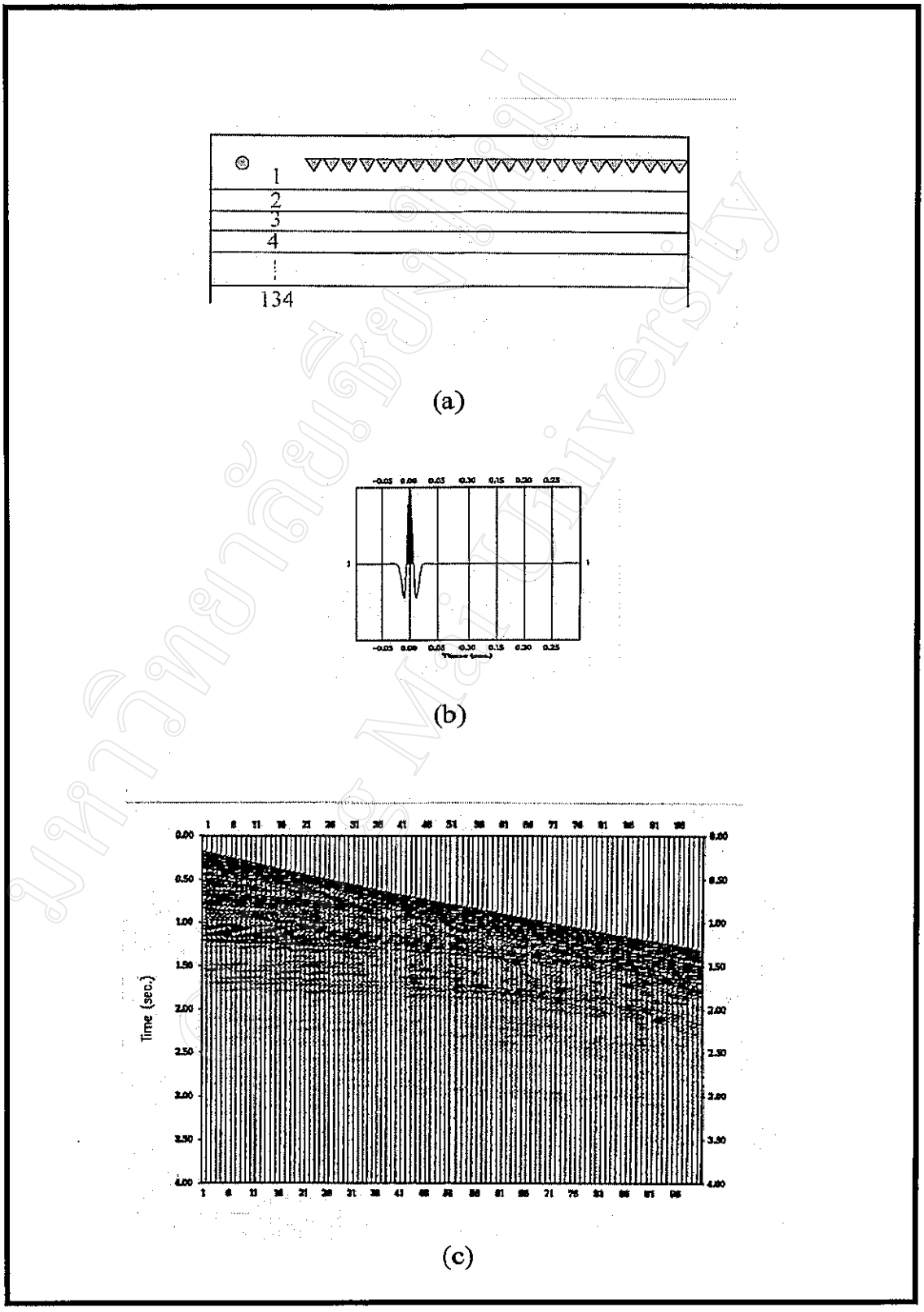

Figure A-4 Marine acquisition simulation by Osiris software involved in this research. Layer-earth model (a) is convolved by (b) Ricker input wavelet for obtaining a modeled shot record (modified from Osiris User's manual, 1993).

Appendix B

Convolution model of multiple

Convolution model multiple

In this appendix, the natures of layered earth, water-reverberation, and ghost are reviewed in terms of their convolution models. The maters are based on Backus (1959), Robinson (1966), Hays (1979), Wardell (1980), Sheriff (1984), Krebes (1989), and Russell (1990).

B.1 *Layered-earth model*

Layered-earth model is a convolution model, which mathematically explains how seismic trace can be produced. The relationship of seismic trace obtained at receiver can be written as:

$$y_t = w_t * x_t + n_t, \quad (1)$$

where y_t , w_t , x_t , n_t , are recorded seismic data, basic seismic wavelet, earth's impulse response or reflectivity series, and random noise, respectively. * denotes a convolution operator. In the experiments, it is assumed the content of noise equal to zero. Thus, its convolution model is then represented by the following equation:

$$y_t = w_t * x_t . \quad (2)$$

B.2 *Water-reverberation model*

Water reverberation within the water layer is examined approximately as a linear filtering. Figure B-1 shows the ray paths of water reverberation in shallow depth model. Let R is a reflectivity coefficient at water-bottom interface. The primary reflection is given the amplitude equal to 1 and has reflected once at sea bottom. The first-multiple (M_1) has bounced twice at the water bottom, hence, its impulse amplitude is $(1)(-R) = -R$. Similarly, the second multiple (M_2) has bounced three times, so the impulse amplitude of $(1)(-R)(-R) = R^2$, and so on. In such circumstance, the reflectivity response of water reverberation, x_t, can be written as

$$x_t = (1,0, ..., 0, -R, 0, ... 0, R^2, 0, ..., 0, -R^3, 0, ...). \quad (3)$$

Since the sum of the geometric series $1 - R + R^2 - R^3 + R^4 ...$,where $|R| < 1$, equals to $1/(1+R)$, equation (3) can be written in z-transform as

$$X(z) = 1/(1+Rz^n) . \quad (4)$$

The seismic trace detected at hydrophone streamer can be modeled by $y_t = w_t * x_t$, thus

$$y_t = w_t - Rw_{t-n} + R^2 w_{t-2n} - R^3 w_{t-3n} + ... \quad (5)$$

Equation (5) is then represented the *water-reverberation model*. They are occurred at time, $t=0$, $n\Delta t$, $2n\Delta t$, and $3n\Delta t$, respectively.

B.3 *Ghost model*

Ghost is defined as energy reflected from the water-air surface before being picked up by a submerged streamer. Consider Figure B-2, let R is a reflection coefficient at water-bottom interface. While the prime pulse is the energy which leaves the source and goes directly downward, it is followed by a ghost pulse, which corresponds to the

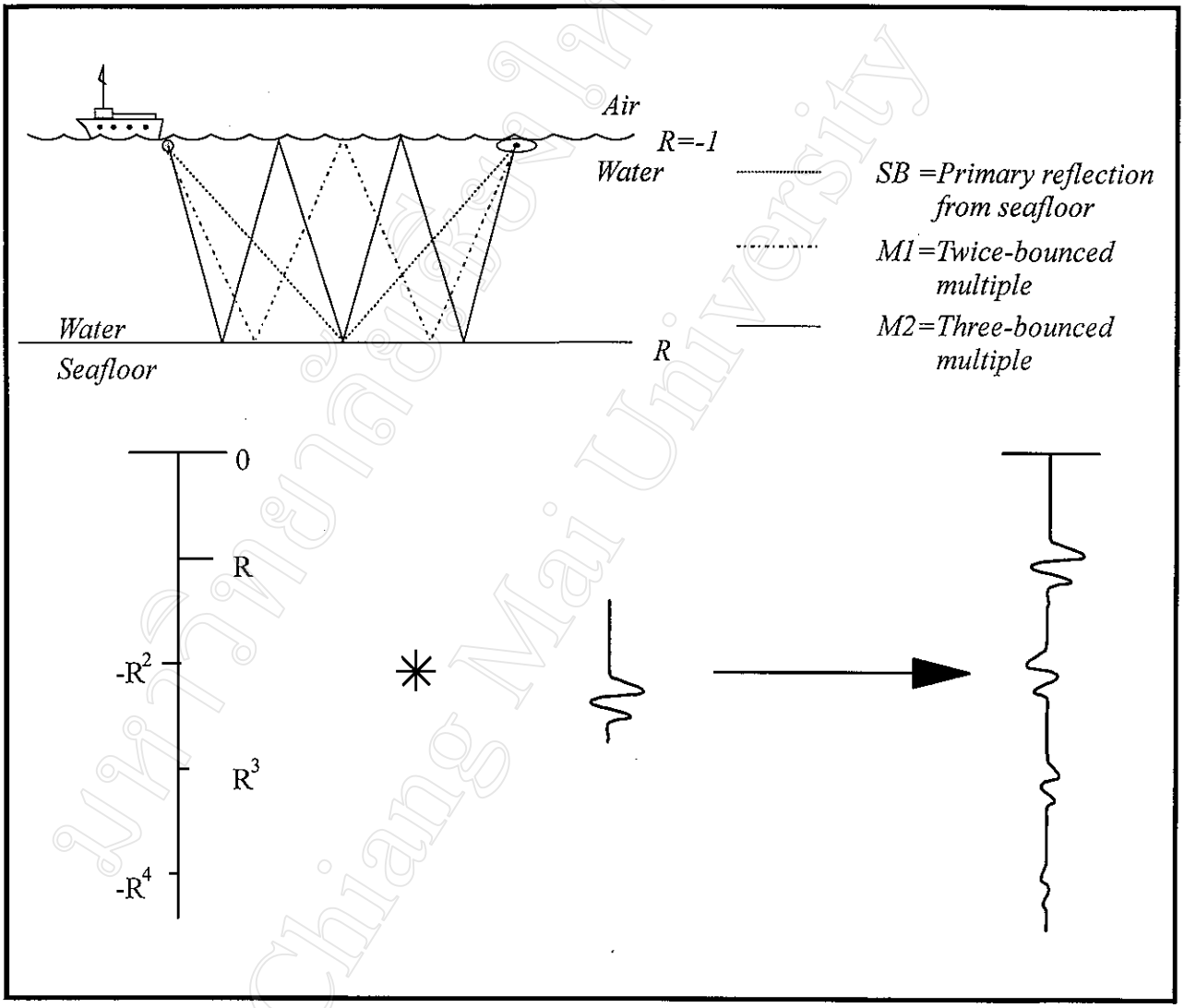

Figure B-1 Water-reverberation model (modified from Hays, 1979)

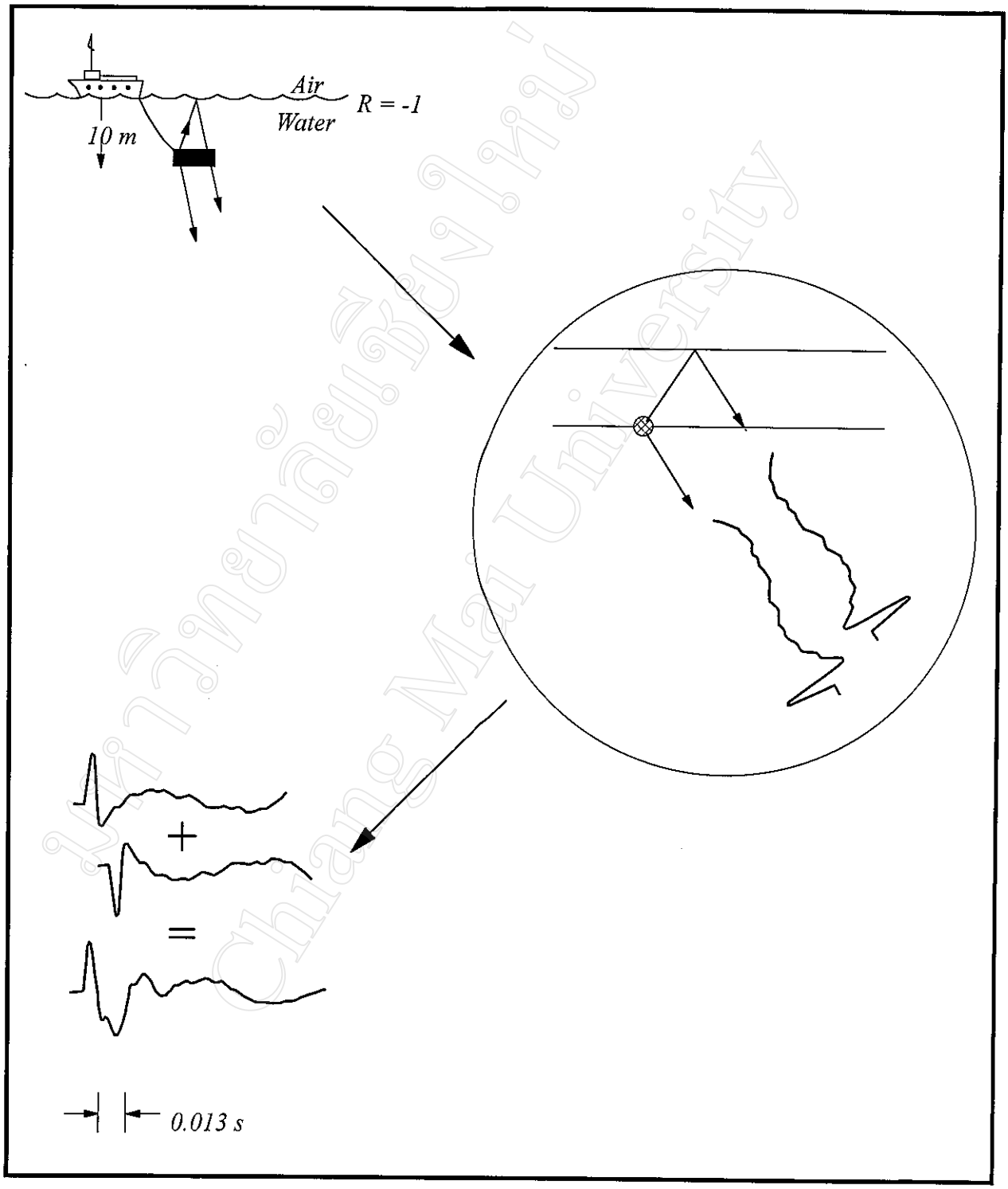

Figure B-2 Ghost model (modified from Wardell, 1980)

energy that travels upward and is then reflected with polarity reversed at the water-air interface The reflectivity series of ghost can be written as:

$x_t = (1, 0, ..., 0, -R)$, or

$X(z) = 1-RZ^n$, $0<R<1$. (6)

R is less than 1 because the ghost loses more energy than the primary. The trace, y_t, contains the ghost can be modeled by

$y_t = w_t - Rw_{t-n}$, (7)

where w_t is the seismic wavelet and x_t is the impulse response of the model. The impulse amplitude are occurred 1 and $-R$ at time, $t = 0$ and $t = n\Delta t$, respectively. This can be written in z-transform as:

$Y(z) = W(z) - W(z)RZ^n$. (8)

The ghost effect makes the sharp prime pulse broadened. The time delay between the prime and the ghost pulses is equal to the two-way travel time, from the shot to the water-air interface. Not only at source end, but ghosting also occurs on the receiver end of reflection travel path.

Appendix C

Review of predictive deconvolution

Review of predictive deconvolution

This mater in this appendix is based Robinson (1957), Peacock and Treitel (1965), Robinson (1966), Sheriff (1984), Yilmaz (1987), Krebes (1989), Russell (1990), Taner and Koehler (1995), and Jakubowicz (1993)

C.1 *Assumptions of deconvolution*

The deconvolution aims to compress wavelet and remove the multiple from seismic data. In these cases, the special working assumptions are required as follows:

Assumption 1 *the earth is made up of horizontal layers of constant velocity*. The source generates a compressional plane wave that impinges on layer boundaries at normal incidence. Under such circumstances, *no shear-wave is generated.*

Assumption 2 the source waveform does not change as it travels in the subsurface. This means *the source wavelet is stationary.*

Assumption 3 *the noise component is zero.*

Assumption 4 Reflectivity is a random process. This implies that the seismogram has seismic wavelet characteristics since their autocorrelation and amplitude spectra are similar. *In brief, the input wavelet is known.*

Assumption 5 *the seismic wavelet is minimum phase*. Therefore, it has a minimum-phase inverse.

C.2 *Approach of deconvolution*

The deconvolution can be subdivided into two general approaches, in term of the source wavelet, *deterministic,* and *statistic deconvolution solution*

1. *Deterministic deconvolution*

This solution can be obtained if the source wavelets are *known* such as the source signal of vibroseis sweep, VSP, designature, or auxiliary recording trace, in these cases, deconvolution works more accurate.

2. *Statistical deconvolution*

This solution can be obtained even if the source wavelet is *unknown* in most of the usual cases. It is commonly applied in the actual processing works.

C3 *Mathematical concept of deconvolution*

The *inverse filter* is the classical operators derived to solve the multiple and ghost problem. Afterwards, it was mathematically developed and modified as follows:

1. Inverse filter

If a seismic trace y_t results from the convolution model between a known wavelet w_t and reflectivity series or earth impulse response w_t, *i.e.*, $y_t = w_t * x_t$, or $Y(z) = W(z)X(z)$. The basic concept of inverse filter is g_t, written as

$$y_t * g_t = x_t, \quad \text{or} \quad Y(z)G(z) = X(z). \tag{1}$$

Substituting equation (10) into seismic convolution model yields

$$g_t = w_t^{-1}, \quad \text{or} \quad G(z) = 1/W(z). \tag{2}$$

By constructing polynomial division or else Taylor expansion, it can be rewritten in time domain, as

$$\delta_t = w_t * g_t = \sum w_i g_{t-i} = w_0 g_t + w_1 g_{t-1} + w_2 g_{t-2} + w_3 g_{t-3} + \ldots,$$

when assumed that w_t and g_t are zero for $t<0$. Solving for g_t yields

$$g_t = 1/w_0(\delta_t - w_1 g_{t-1} - w_2 g_{t-2} - \ldots - w_n g_{t-n}), \quad (3)$$

for $n+1$ term wavelet. This formula allows us to compute g_t recursively, i.e.,

$$g_0 = 1/w_0\,,\ g_1 = -(w_1/w_2)g_0\,,\ g_2 = -1/w_0(w_1 g_1 + w_2 g_0)\,,\ \ldots \quad (4)$$

To obtain directly the deconvolution output trace x_t, i.e., reflection coefficient series, replacing g_t with x_t and δ_t with y_t in equation (3), this gives

$$x_t = 1/w_0(y_t - w_1 y_{t-1} - w_2 y_{t-2} - \ldots - w_n y_{t-n}) \quad (5)$$

Equation (5) is the result of an inverse filter applied to y_t to obtain x_t. This type of filter is known as *recursive inverse filtering* or *feedback filtering*. The x_0 is fed back into equation (5) to obtain x_1, then x_0 and x_1, are fed back to obtain x_2, and so on.

2. Prediction operator and Prediction error operator

Although the inverse filter works well, the truncated finite term filter caused some errors in the deconvolved result. Therefore, a prediction operator and a prediction error operator were developed to obtain an optimum filter, which is effective with as less error as possible.

A prediction operator, if a_t is a filter with prediction distance α, the output y_τ will be an estimate of the input x_t at some future time $t+\alpha$. Consider the output y_t, it can be obtained from the discrete convolution between the input x_t and the inverse filter a_t and can be written

$$y_\tau = \Sigma\, x_t a_{\tau-t} = x'_{t+\alpha}\,, \quad (6)$$

where $x'_{t+\alpha}$ is an estimate of $x_{t+\alpha}$.

An error series, $\in_{t+\alpha}$, is defined as the difference between the actual value $x_{t+\alpha}$ and the estimated or predictive value $x'_{t+\alpha}$. This gives

$$\in_{t+\alpha} = x_{t+\alpha} - x'_{t+\alpha}. \quad (7)$$

Thus, $\in_t$ is an output series, which represents an unpredictable part of x_t. Substituting (6) in (7) results in

$$\in_{t+\alpha} = x_{t+\alpha} - \Sigma\, x_t a_{\tau-t} \quad \text{or} \quad z^{-\alpha}E(z) = z^{-\alpha}X(z) - X(z)A(z). \quad (8)$$

Multiplication of both side of equation (8) by $z^{-\alpha}$ yields

$$E(z) = X(z)[1 - z^{-\alpha}A(z)]. \quad (9)$$

The term $[1 - z^{-\alpha}A(z)]$ is the z-transform of the so-called *prediction error operator*. It is defined as the difference between the zero-delay unit spike and the prediction operator, $A(z)$, delayed by the prediction distance

Suppose that the prediction operator, a_t, is given by the n-length series, i.e.,

$$a_t = a_0, a_2, \ldots, a_{n-1}.$$

So the corresponding *prediction error operator*, $f_{\tau-t}$ with prediction distance α is

$$f_t = 1, 0, 0, 0, \ldots., 0, -a_0, -a_1, \ldots, -a_{n-1}. \quad (10)$$

$$|\ldots\alpha\text{-}1 \text{ zeros}|$$

The terms, between 1 and $-a_0$, are predictable portion of such a trace and then zeroed out.

3. Least-square inverse filter

Definitely, it is the filter for which the sum of the squares of the errors is a minimum. In general, the least-squares filter involves the three signals, namely the *input signal*, the *desired output*, and the *actual output signal*.

Let x_t = input $= (x_0, x_1)$, f_t = filter $= (f_0, f_1)$, and d_t = desired output = (d_0, d_1, d_2), The actual output y_t resulted from the convolution between x_t and the filter f_t is

$$y_t = x_t * f_t = (x_0 f_0,\ x_0 f_1 + x_1 f_0,\ x_1 f_1), \tag{11}$$

The minimization of the energy, J, is the difference between the desired output d_t and the actual output y_t, i.e.,

$$J = \Sigma (d_t - y_t)^2 = 2(d_0 - x_0 f_o)^2 + (d_1 - x_0 f_1 - x_1 f_0)^2 + (d_2 - x_1 f_1)^2. \tag{12}$$

The partial derivative of J is taken to obtain the least-squares filter f_t, and reduced the form to

$$\begin{aligned} (x_0^2 + x_1^2) f_o + (x_0 x_1) f_1 &= x_0 d_0 + x_1 d_1 \\ (x_0 x_1) f_0 + (x_0^2 + x_1^2) f_1 &= x_0 d_1 + x_1 d_2 . \end{aligned} \tag{13}$$

Assuming that x_t and y_t are real-valued signals and recalling the definition of the crosscorrelation, $\Phi_{xy}(t) = \Sigma\, x_t y_{t+\tau}$, equation (13) can be written as

$$\begin{aligned} \Phi_{xx}(0) f_o + \Phi_{xx}(1) f_1 &= \Phi_{xd}(0) \\ \Phi_{xx}(1) f_o + \Phi_{xx}(0) f_1 &= \Phi_{xd}(0). \end{aligned} \tag{14}$$

These are known as the *normal equations*. For $n = 1$ term, it can be put into the matrix form, i.e.,

$$\begin{bmatrix} r_0 & r_1 \\ r1 & r_0 \end{bmatrix} \begin{bmatrix} f_0 \\ f_1 \end{bmatrix} = \begin{bmatrix} g_0 \\ g_1 \end{bmatrix} . \tag{15}$$

For any n length, the matrices can be presented as

$$\begin{bmatrix} r_0 & r_1 & r_2 & \cdots & r_{n-1} \\ r_1 & r_0 & r_1 & \cdots & r_{n-2} \\ r_2 & r_1 & r_0 & \cdots & r_{n-3} \\ & & \vdots & & \\ r_{n-1} & r_{n-2} & r_{n-3} & \cdots & r_0 \end{bmatrix} \begin{bmatrix} f_0 \\ f_1 \\ f_2 \\ \\ f_{n-1} \end{bmatrix} = \begin{bmatrix} g_0 \\ g_1 \\ g_2 \\ \\ g_{n-1} \end{bmatrix} , \tag{16}$$

where $r_{t,}$ the symmetrical autocorrelation matrix at left called a *Toeplitz matrix*, is the autocorrelation of the input, f_t is the least-square filter, and g_t is the crosscorrelation between input and the desired output. The crosscorrelation column matrix on the right side is made up of lags of correlation.

4. Predictive deconvolution

Consider the prediction process as it relates to a seismic trace. A time series x_t can be predicted at a future time $t+\alpha$, where α is the prediction lag (or prediction distance). An autocorrelation of seismic trace generally consists of two parts, *predictable* and *unpredictable*. A predictable part contains a predictable component (multiples) with a periodic rate occurrence. While an unpredictable part contains genuine reflections and random noise since they are unsystematic.

The filter a_t used to estimate $x_{t+\alpha}$ could be computed by using a special form of the matrix equation. Since the desired output $x_{t+\alpha}$ is the time-advanced version of the input x_t, the right side of equation (16) is the specialized for the prediction problem. Equation (17) for the case of an n-long prediction filter and a α-long prediction lag can be generalized,

$$\begin{bmatrix} r_0 & r_1 & r_2 & \dots & r_{n-1} \\ r_1 & r_0 & r_1 & \dots & r_{n-2} \\ r_2 & r_1 & r_0 & \dots & r_{n-3} \\ \vdots & \vdots & \vdots & \dots & \vdots \\ r_{n-1} & r_{n-2} & r_{n-3} & \dots & r_0 \end{bmatrix} \begin{bmatrix} a_0 \\ a_1 \\ a_2 \\ \vdots \\ a_{n-1} \end{bmatrix} = \begin{bmatrix} r_\alpha \\ r_{\alpha+1} \\ r_{\alpha+2} \\ \vdots \\ r_{\alpha+n-1} \end{bmatrix} . \qquad (17)$$

For deconvolution operator, in practical, only extracting the seismic wavelet and finding its inverse would be done. However, if some zero frequencies in amplitude spectrum are inversed, it will cause an unstability of the operator. To make the inverse more stable, the prewhitening is then typically specified in the prediction filter, both spiking and predictive deconvolution.

Prewhitening, ε means adding a small amount of white noise to the trace and boosting its amplitude spectrum by a small constant amount at all frequencies, before the filter is obtained and applied. It is achieved by adding a constant to the zero lag of the autocorrelation function.

In dealing with removing multiple, there are four basic parameters to be examined before applying predictive deconvolution, *gate length of autocorrelation (G)*, *operator length (n)*, *prediction distance or gap length* (α), and *amount of white noise* or *percentage of prewhitening* (ε). In practical, analysis of autocorrelation of input trace in Figure C-1 is used as a key for designing these parameters. Computation for predictive deconvolution can be subdivided into three main steps. *The first step* is to compute the autocorrelation function of that portion of the sampled trace with in a specified time gate. *The second step* is to compute the coefficients of the *prediction operator* a_t, and the *prediction error operator,* f_t, which requires inverse operator for deconvolving the seismic trace x_t. *The third step* is to convolve the prediction error operator, f_t, with the seismic trace, x_t. This computation is carried out according to the discrete convolution formula. The result is the prediction error series (for prediction span α), which represent the deconvolved (but uncleaned) seismic trace. By this way, the reverberation is eliminated from each of the waveform w_t, but leave intact the initial nonreverberation portions, while increasing seismic resolution. Filtering steps used are illustrated in Figure C-2.

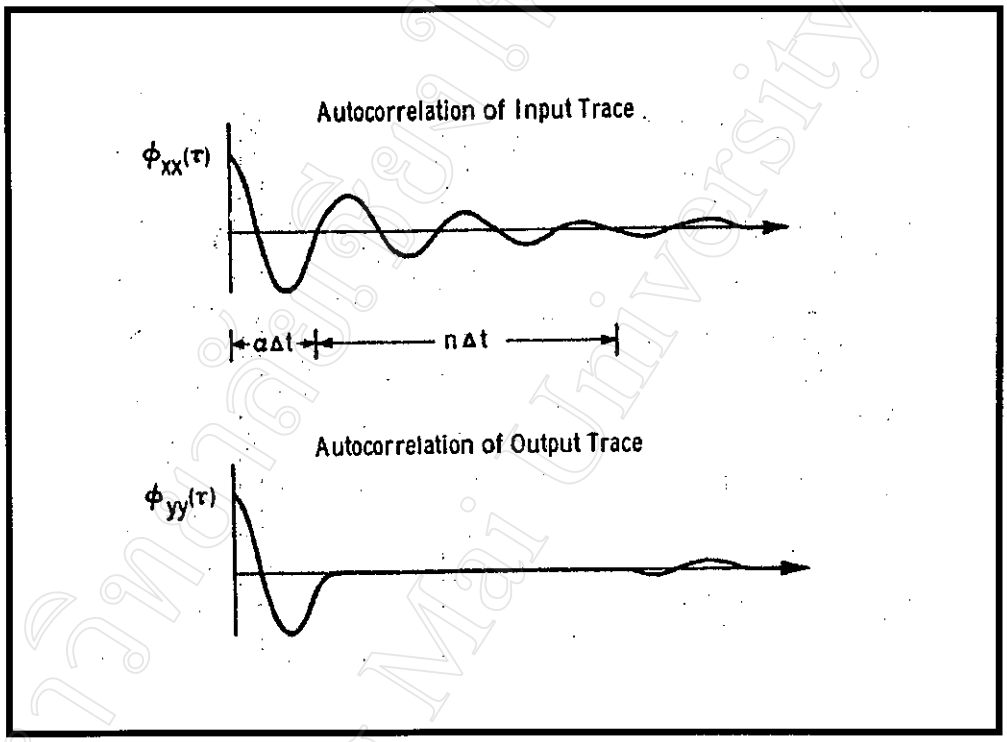

Figure C-1 Analysis of autocorrelation of input trace used for designing the parameter of filter (Peacock and Treitel, 1967)

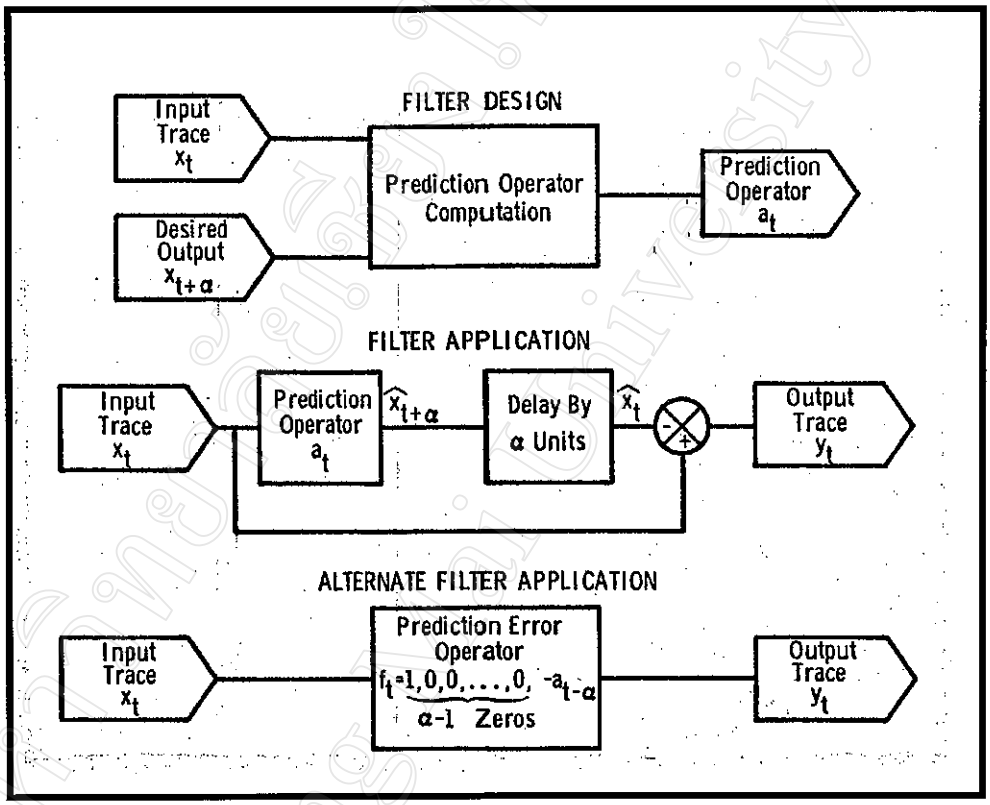

Figure C-2 Predictive filtering in concept (modified from Peacock and Treitel, 1976)

Appendix D

Test of muting and *NMO*/*DNMO* effect

Testing of mute and *NMO/DNMO* effect

Front-end mute as a surgery cutter, and a package of *NMO/DNMO* as the non-linear algorithm, had to be checked their effects whether they would change the characteristic of seismic data or not. It could be done on the modeled shot since they were applied to the modeled data in preparation stage for obtaining the suitable condition of deconvolution.

Locating the reject area cover the first break signal, the front-end mute was applied. Figure D-1 shows the results of modeled shots with their corresponding autocorrelation. There was slightly different on shots modeled shot at only near and far traces, whereas only the part of first break and refracted wave were zeroed out. The contrast of them could be detected as the yellow color on the overlay plot in Figure D-2. It can be concluded that the data was not changed by the mute since main data was still be existed while the change was concentrated only in the muted zone.

NMO and *DNMO* were later tested. Using the multiple velocity of 1,500 m/s, applying *NMO* and then reversing by *DNMO*, the output on shot were illustrated on Figure D-3 and D-4. All curvatures of primary and multiples were not much transformed whereas the linear events of direct- and refracted wave were partially changed. The autocorrelations confirmed that there were slightly altered from the escaping of the linear events as seen in Figure D-3. The blue color in Figure D-4 meant somewhat disappeared caused by the non-linear process. Note that the blue color was assembled at only the upper time of the modeled shot.

NMO/Mute/DNMO were thus tested. Using the multiple velocity of 1,500 m/s, applying *NMO*, muting by the same mute function for keeping constant, and then reversing by *DNMO*, the output on shot were illustrated on Figure D-5 and D-6. All curvatures were a little change especially at the upper time whereas it was ultimately zeroed in stage of post-NMO mute in an actual work.

It could be proved here that the model data was acceptable since most of the hyperbolae still be the same. However, the linear of refraction data could be ignored because, in fact, it is the unwanted noise normally cut off in usual works.

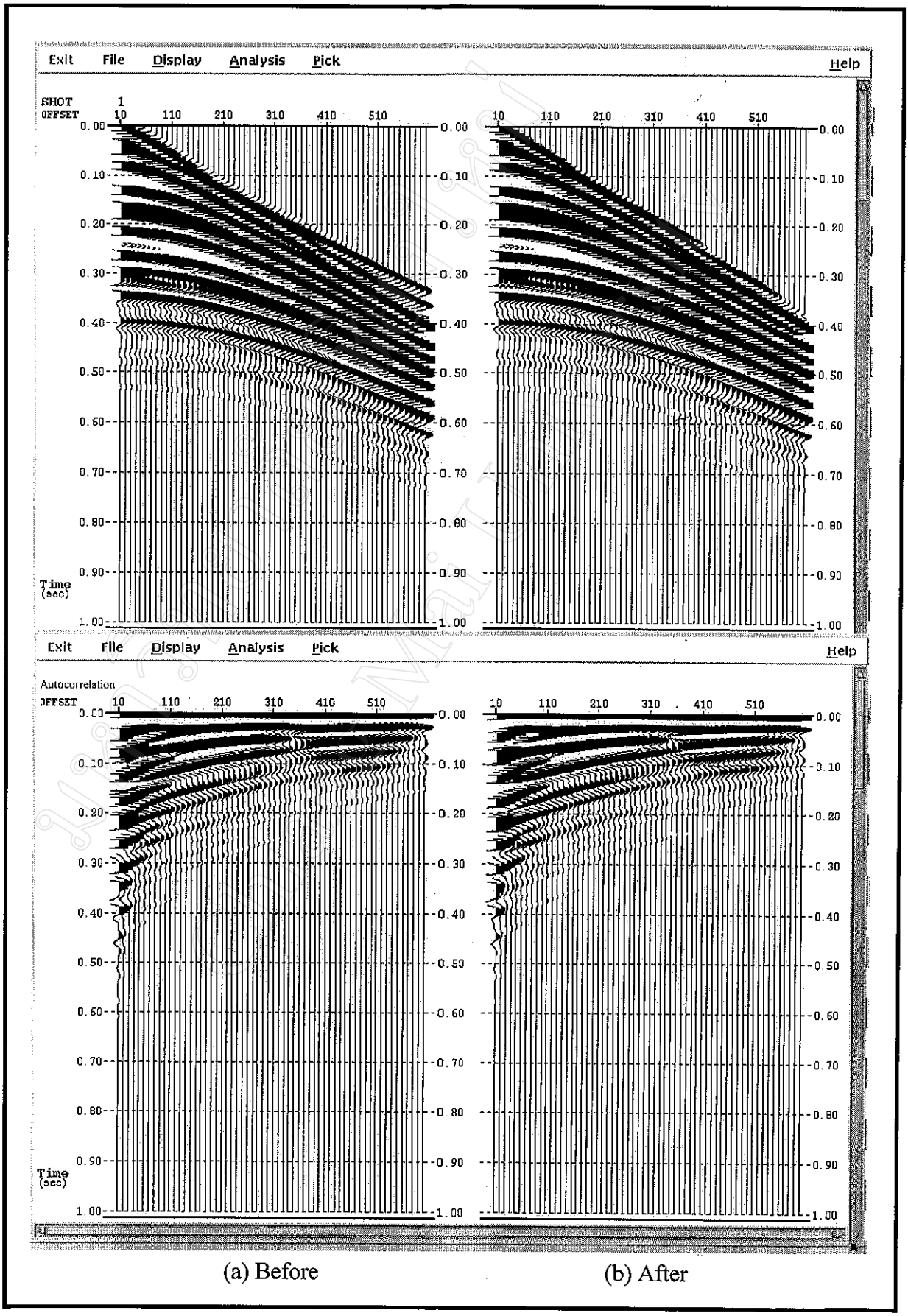

Figure D-1 Test of mute effect

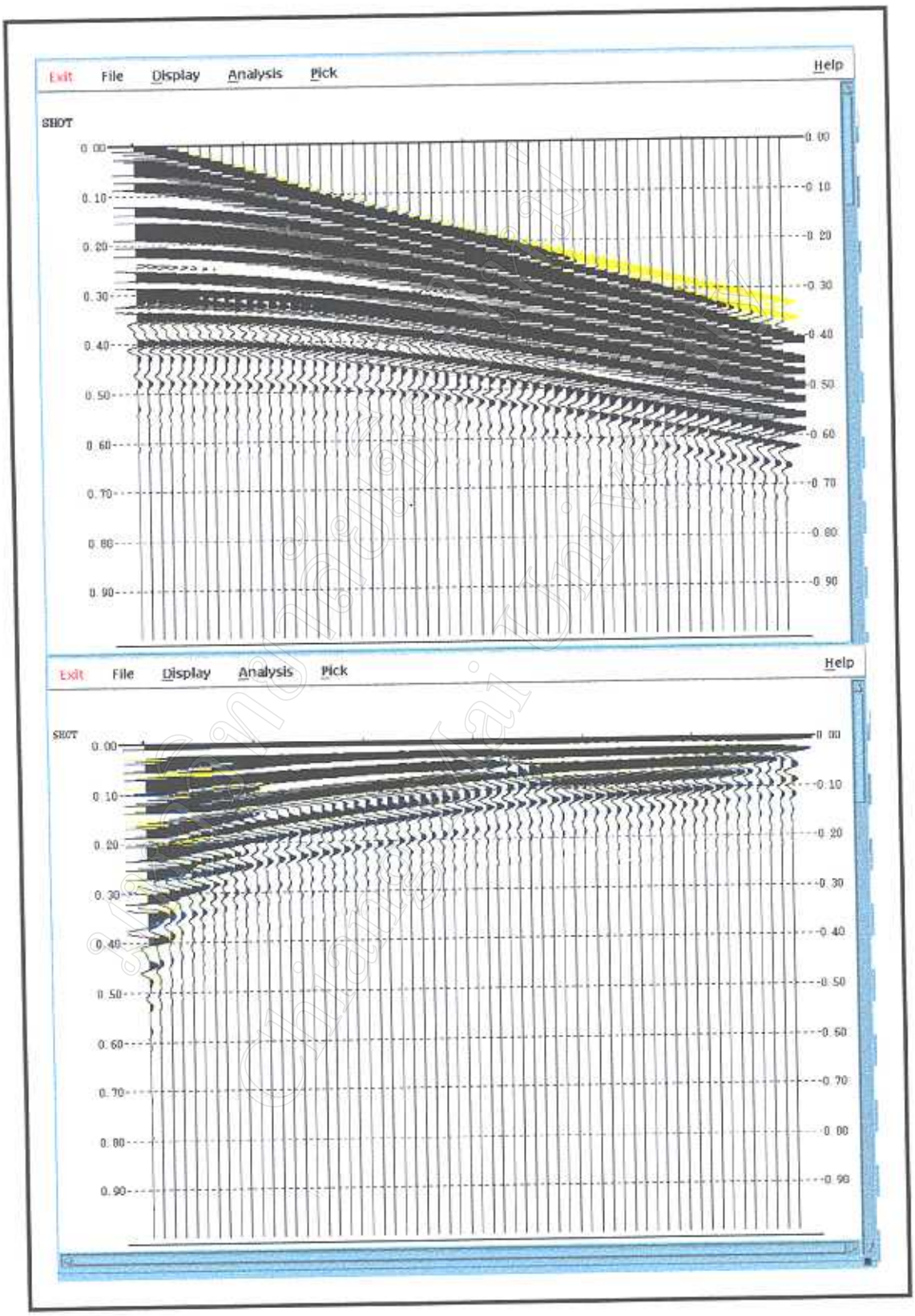

Figure D-2 Overlay plots of modeled shot and their corresponding autocorrelations before (yellow) and after (blue) mute was applied. The difference is justified in yellow color.

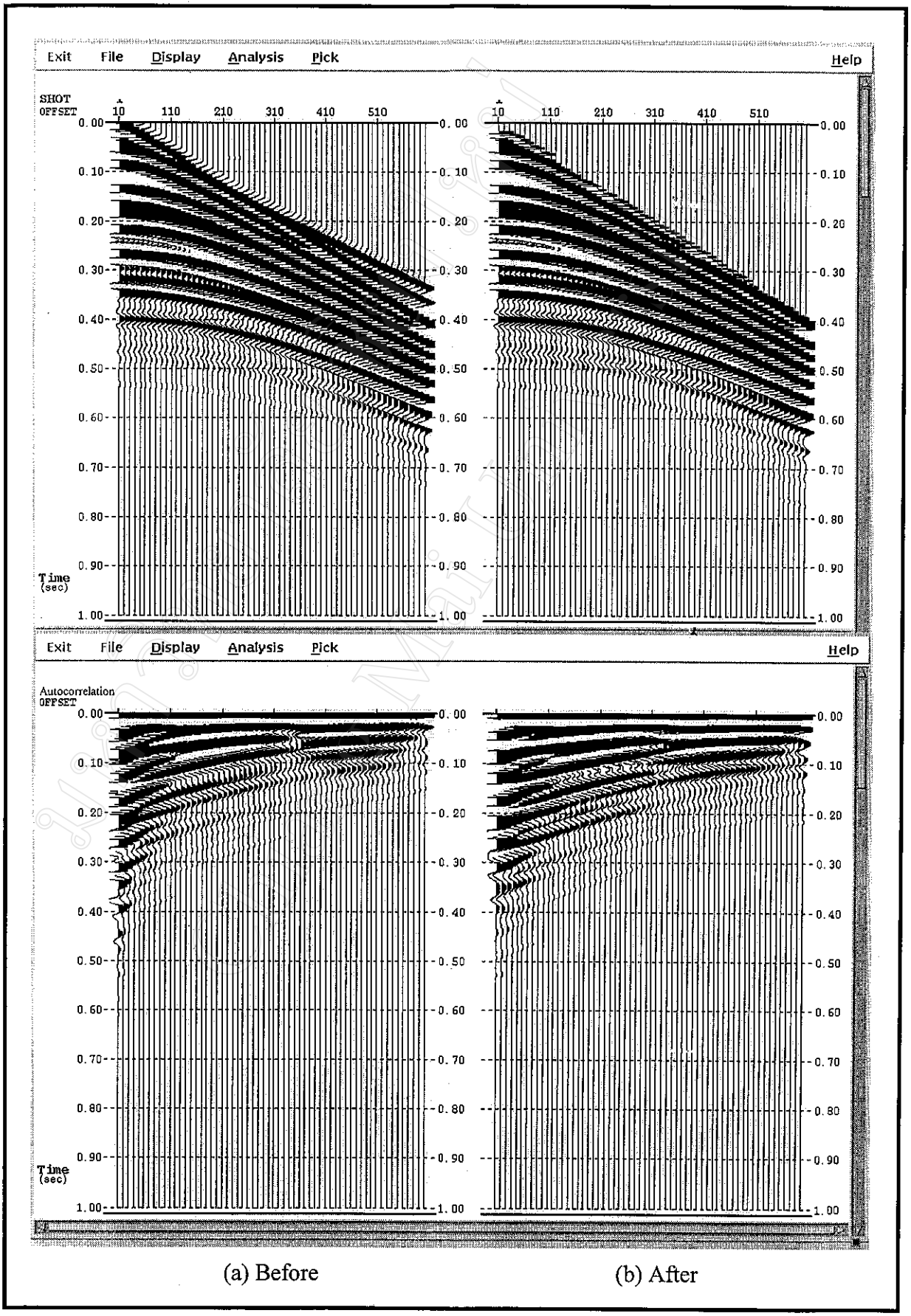

Figure D-3 Test of NMO/DNMO effect

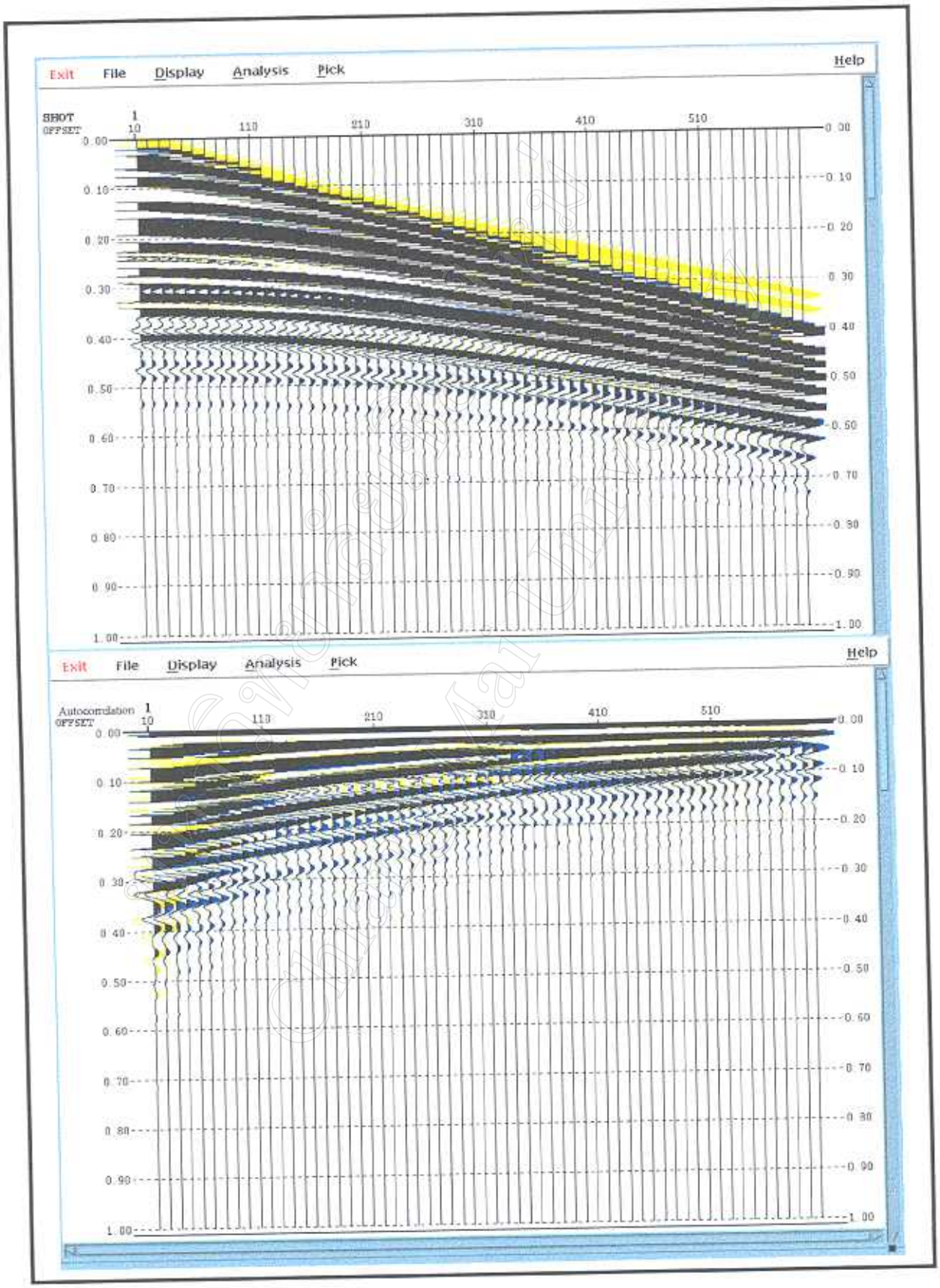

Figure D-4 Overlay plots of modeled shots and their corresponding autocorrelations before (yellow) and after (blue) *NMO/DNMO* were applied. The difference is justified in yellow color.

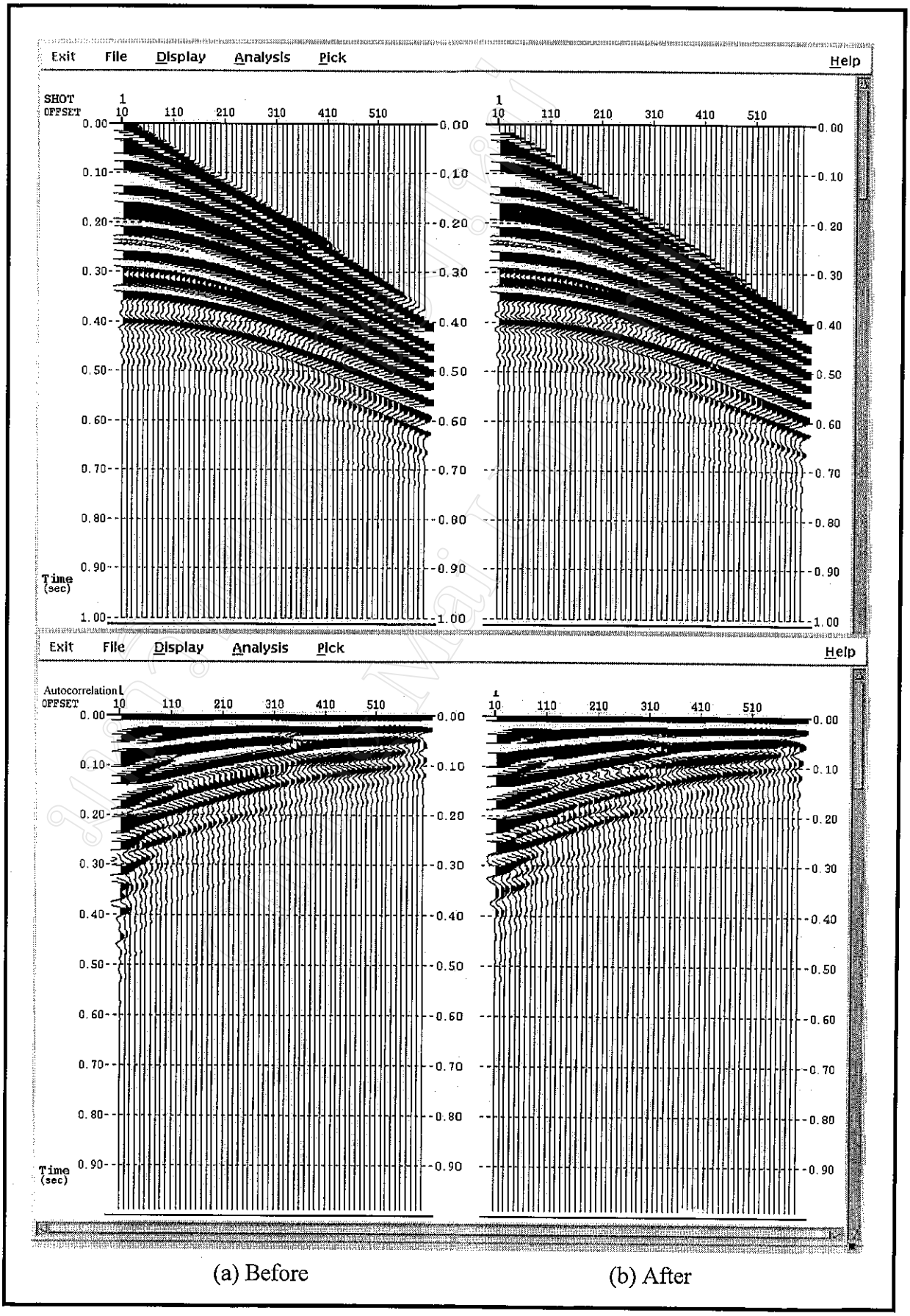

Figure D-5 Test of *NMO/MUTE/DNMO* effect

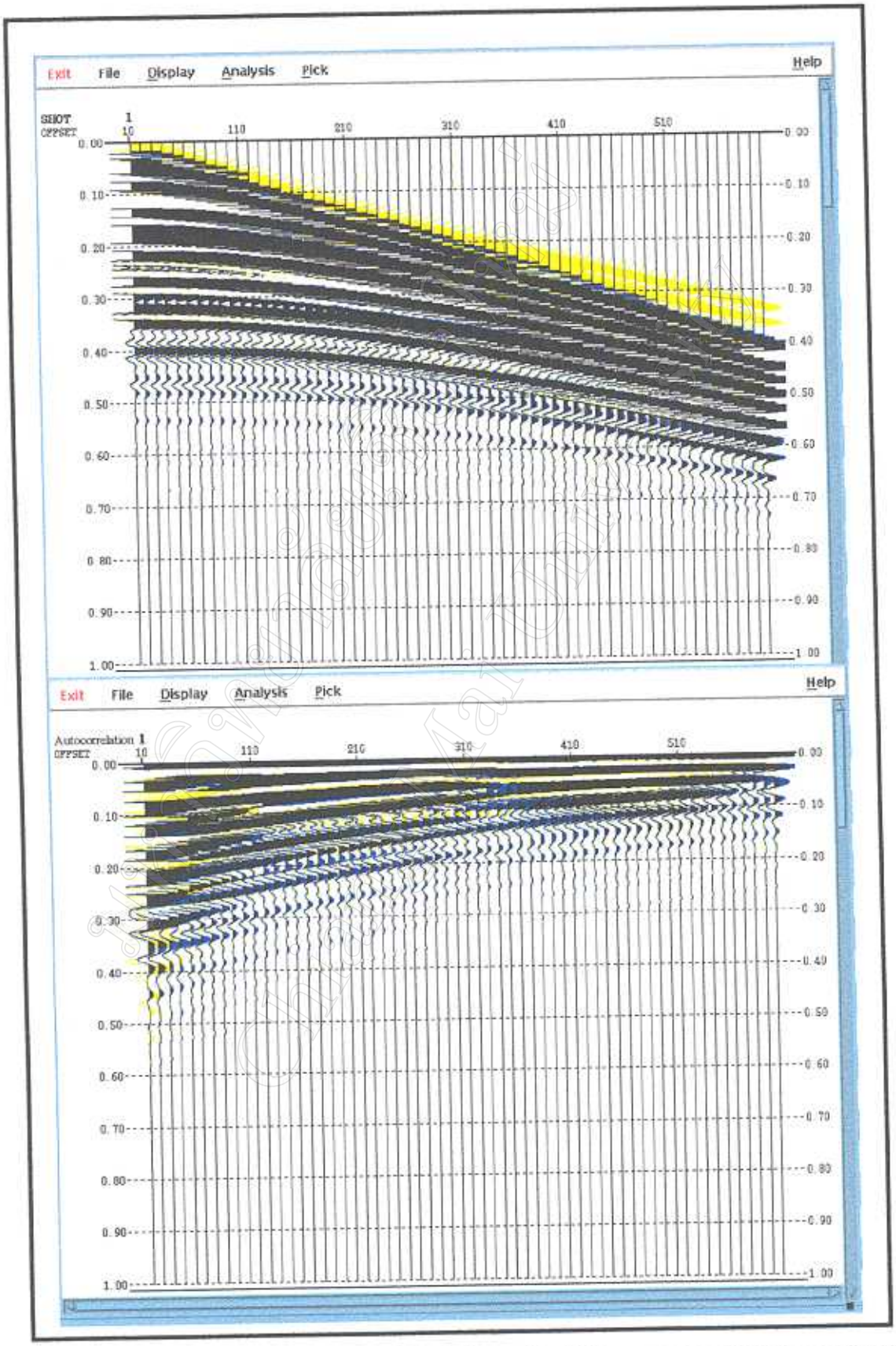

Figure D-6 Overlay plots of modeled shots with their corresponding autocorrelations before (yellow) and after (blue) *NMO/MUTE/DNMO* were applied. The difference is justified in yellow color.

Appendix E

Test of predictive deconvolution parameters

Test of predictive deconvolution parameters

Deconvolution always deals with assigning parameters and applying to the seismic data. To meet a goal of deconvolution, the designing parameters have to be tested to ensure obtaining the optimum ones.

There were four important parameters in this account, (a) an autocorrelation gate, *G*, (b) an *operator length*, *n*, (c) a *gap length* or *prediction distance*, α, and (d) a *percent prewhitening*, ϵ. Following the method of Yilmaz (1987), fixing three variables while varying only one variable was the method used. A preliminary test, Figure E-1, shows that testing parameters after *NMO* correction gives a clearer feature than ordinary shot and easy to observe what was changed. Thus, all testing will be performed and kept displaying in this way.

Firstly, autocorrelation gate *G*, was tested. Consider the autocorrelation of the modeled shot record in Figure E-1 (b), first-and second-zero crossing were 8 and 24 millisecond, respectively. In such circumstance, α = 8 ms, operator length, n = 400 ms, ϵ = 0.01 were firstly fixed as dummy parameters while autocorrelation gate was planed to be varied from small to large. The results in Figure E-2 shows that the *G* of 1,000 ms in length yielding a good performance and not much great different if increasing the gate more than this. Therefore, the *G* value of 1,000 ms is the optimum gate length in this test.

Secondly, fixing *G* of 1,000 ms, α of 8 ms and ϵ of 0.1 %, *n* was varied form a small value of 50 ms to a large value of 400 ms. The result, in Figure E-3 show that the *n* value of 84 ms gives the best quality. Shorter than this length, the quality is low while longer than this length, it does not show the particular performance. So that, the *n* value of 84 ms is the optimum in this test.

Thirdly, fixing *G* of 1,000 ms, *n* of 84 ms, together with the ϵ = 0.1 %, α value was then varied from 4 ms to 80 ms. The results in figure E-4 shows that the α value of 24 ms yielding the best quality. Shorter than this length, the quality is low while longer than this length, the quality does not show the particular performance. Therefore the α value of 24 ms, which is equal to the second zero crossing, was the optimum operator length in this test.

Lastly, fixing *G* of 1,000 ms, n = 84 ms, and α = 24 ms, ϵ was varied from 0.01 to 1 %. There was nothing significant in any cases even using high or low percent prewhitening. In this case, it was reasonable to select only a small value of 0.1 % representative the percentage of prewhitening in this research.

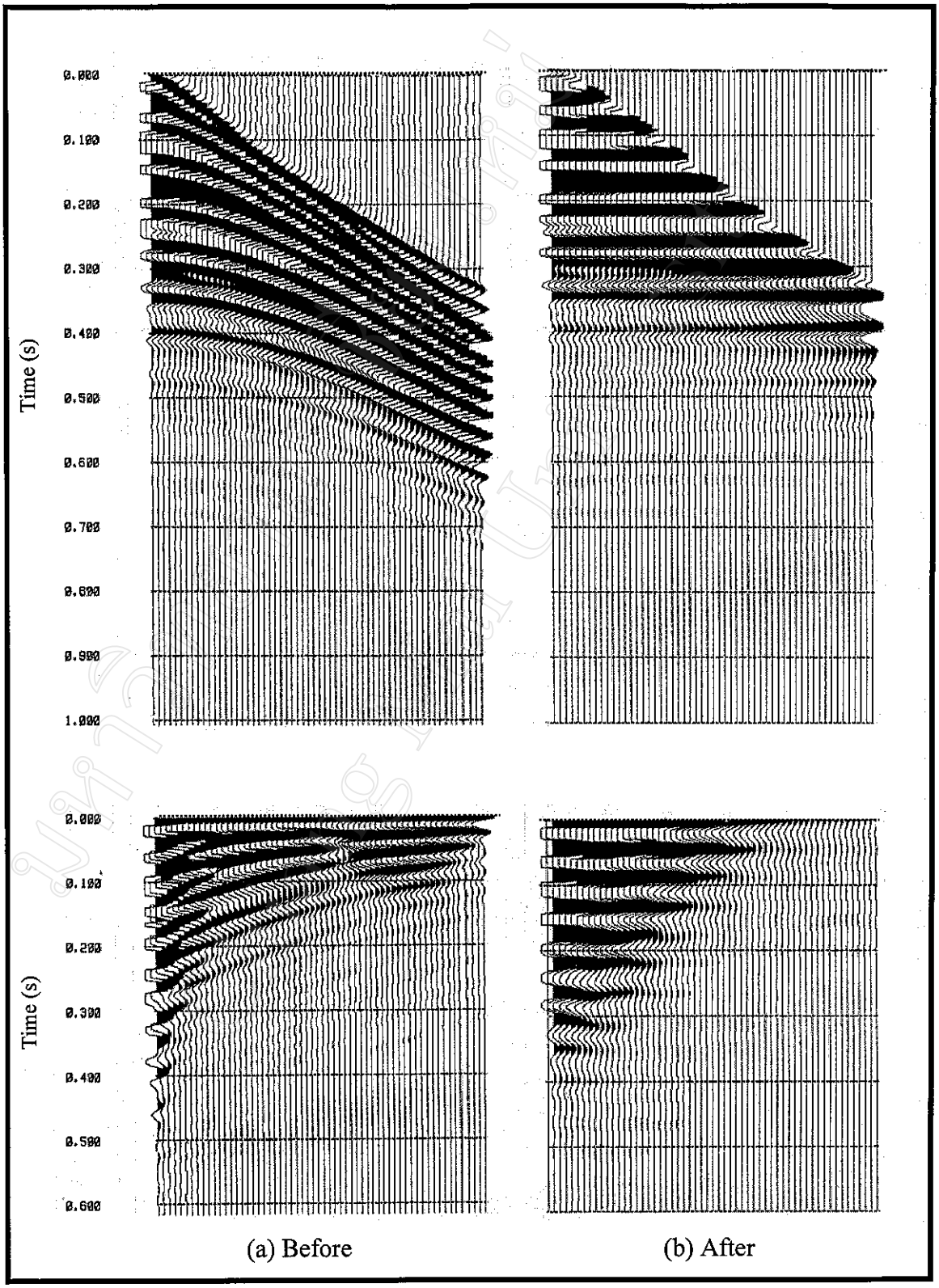

Figure E-1 Modeled shot before and after being applied NMO correctionwith their corresponding autocorrelation at below

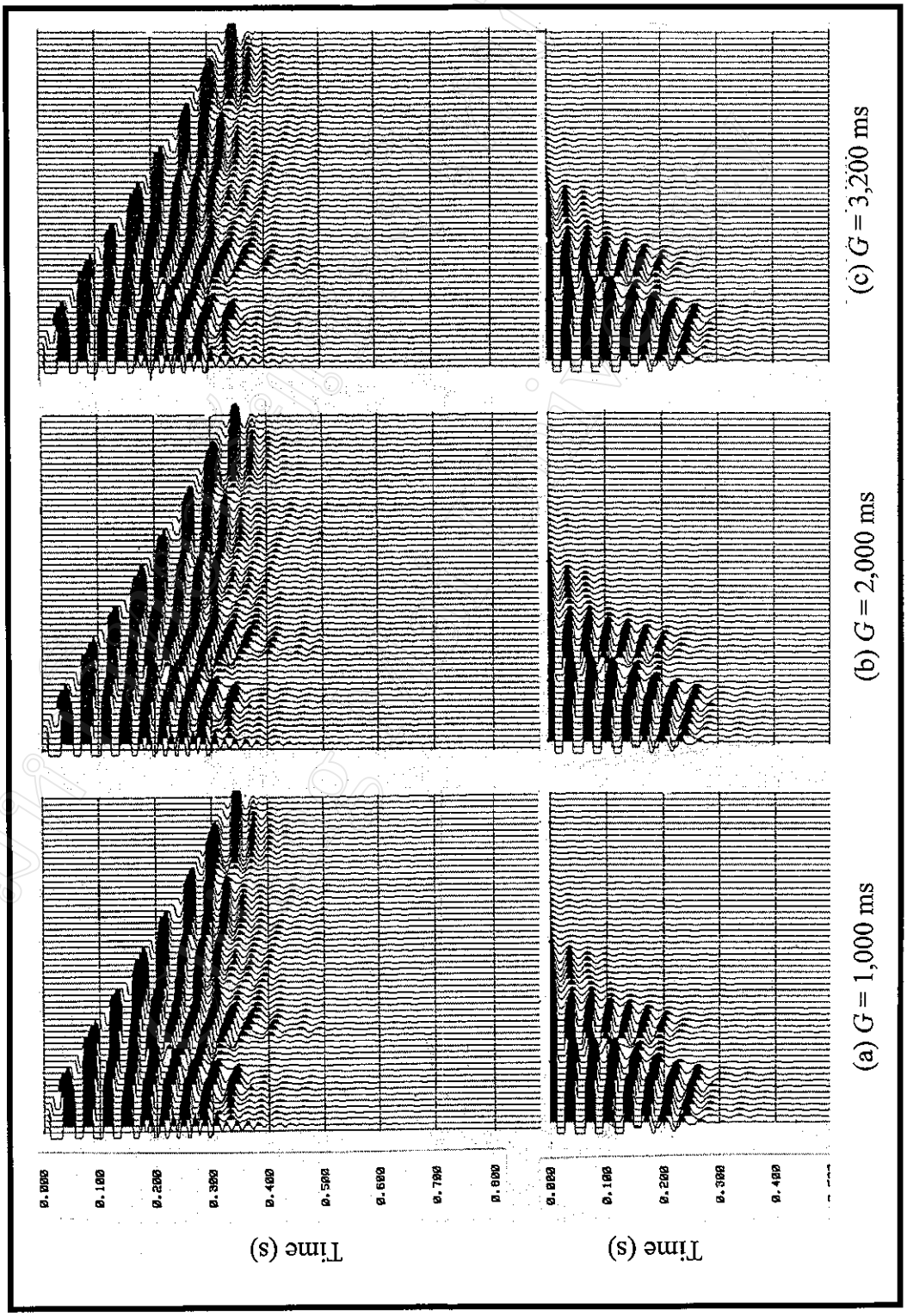

Figure E-2 Test of autocorrelation gate (G) on modeled shot, where α = 24 ms, n = 400 ms and ε = 0.1 %

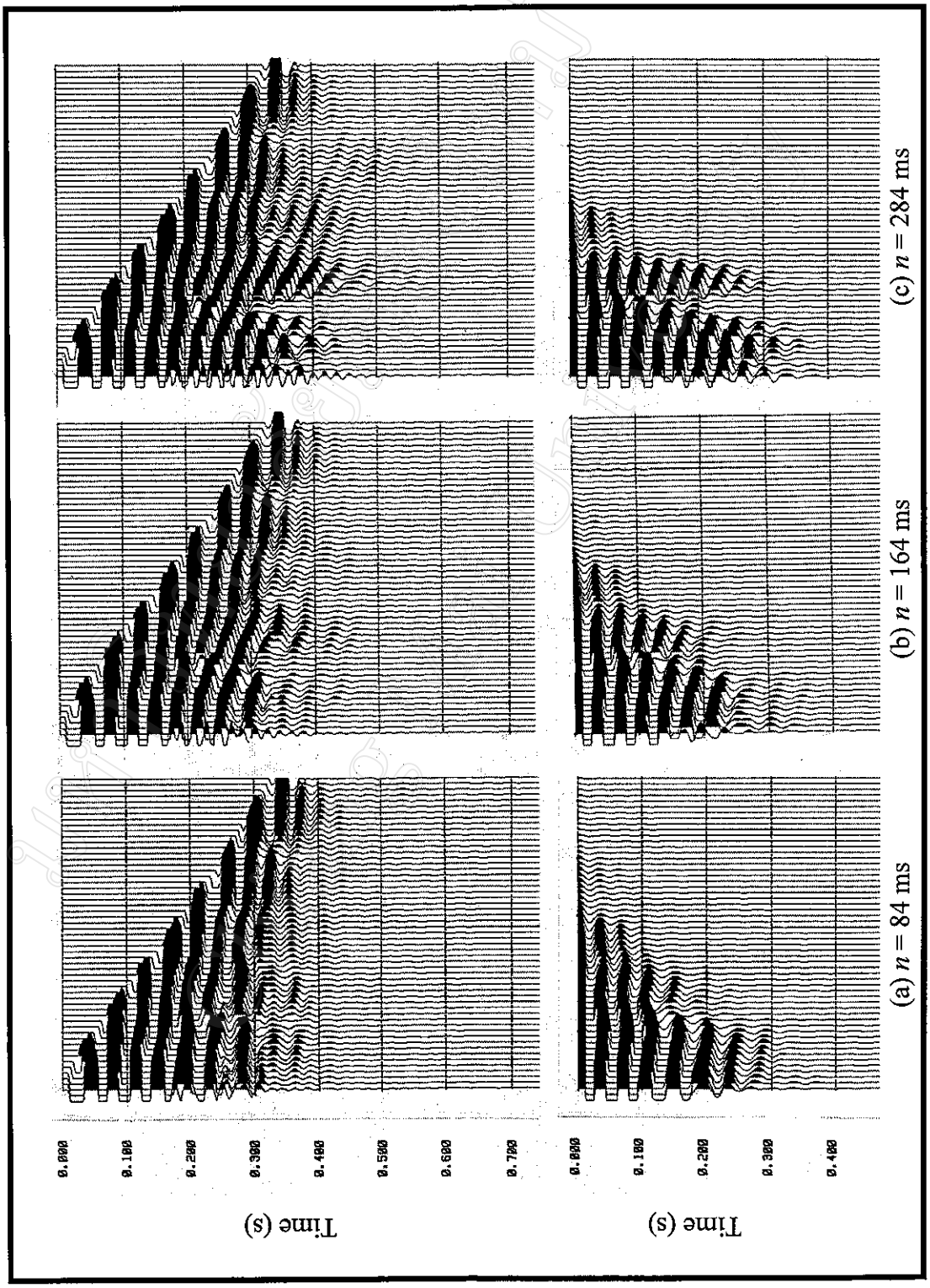

Figure E-3 Test of operator length (n) on modeled shot, where α = 24 ms, G = 1,000 ms and ε = 0.1 %

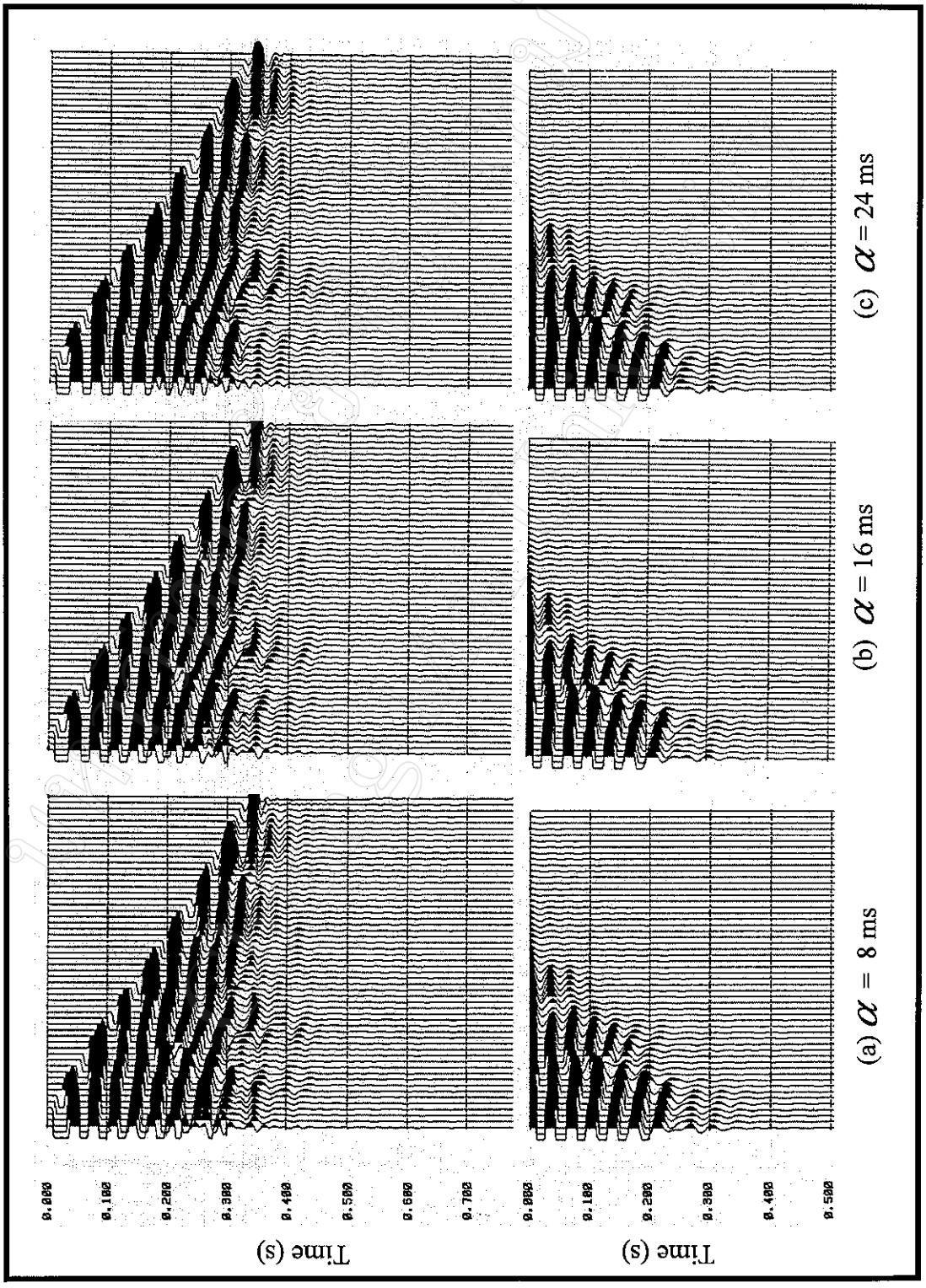

Figure E-4 Test of prediction distance (α) on modeled shot, where G = 1,000 ms, n = 164 ms and ε = 0.1 %

Curriculum Vitae

Noppadol Poomvises earned his B.S. in geology from Chiang Mai University in 1984 and his M.S. in Applied Geophics Program from Chiang Mai University in 1999. His undergraduate research was in geotechnical topic while his master research was in geophysical seismic data processing.

He has been working for the Royal Irrigation Department (RID), Ministry of Agrricultural and Cooperatives since 1984. Between 1985 and 1986, he worked as well-site and engineering geologist on several projects in Thailand. Between 1987 and 1990, he worked as geophysicist and 1991 to 1993 as geotechnical geologist. During 1994 to 1995, he left for two years in order to study for his master's degree and backed to his work at RID since 1996.

Shortly after returning, he was promoted to be chief of 2nd geotechnical investigation party which was involved in geophysical and geotechnical investigation.